

## Supplementary Information

### Design of Amorphous ZnWSe<sub>2</sub> Alloy-based Counter Electrode for Highly Efficient Dye-Sensitized Solar Cells

D. A. Ari<sup>1</sup>, A. Sezgin<sup>1</sup>, M. Unal<sup>1</sup>, E. Akman<sup>2</sup>, I. Yavuz<sup>3</sup>, F. C. Liang<sup>4</sup>, M. Yilmaz<sup>1,5\*</sup>, S. Akin<sup>1,6\*</sup>

<sup>1</sup> Laboratory of Advanced Materials & Photovoltaics (LAMPs), Necmettin Erbakan University, 42090, Konya, Turkey

<sup>2</sup> Scientific and Technological Research and Application Center, Karamanoglu Mehmetbey University, 70200, Karaman, Turkey

<sup>3</sup> Department of Physics, Marmara University, Ziverbey, 34722, Istanbul, Turkey

<sup>4</sup> Institute of Organic and Polymeric Materials, Research and Development Center of Smart Textile Technology, Taipei University of Technology, 10608, Taipei, Taiwan, China

<sup>5</sup> Department of Fundamental Sciences, Necmettin Erbakan University, 42090, Konya, Turkey

<sup>6</sup> Department of Metallurgical and Materials Engineering, Necmettin Erbakan University, 42090, Konya, Turkey

\*E-mail(s): [mucahityilmaz@erbakan.edu.tr](mailto:mucahityilmaz@erbakan.edu.tr) (M. Yilmaz); [seckinakin@erbakan.edu.tr](mailto:seckinakin@erbakan.edu.tr) (S. Akin)

**Table S1.** The growth parameters of CE films.

Sample abbreviation	RF Power of Zn (Watt/cm <sup>2</sup> )	RF Power of WSe <sub>2</sub> (Watt/cm <sup>2</sup> )	Power ratios of Zn and WSe <sub>2</sub> targets
WSe <sub>2</sub>	0	4.3	0
ZnWSe <sub>2</sub> -1	0.27	4.3	1/16
ZnWSe <sub>2</sub> -2	0.54	4.3	1/8
ZnWSe <sub>2</sub> -3	1.08	4.3	1/4
ZnWSe <sub>2</sub> -4	2.15	4.3	1/2

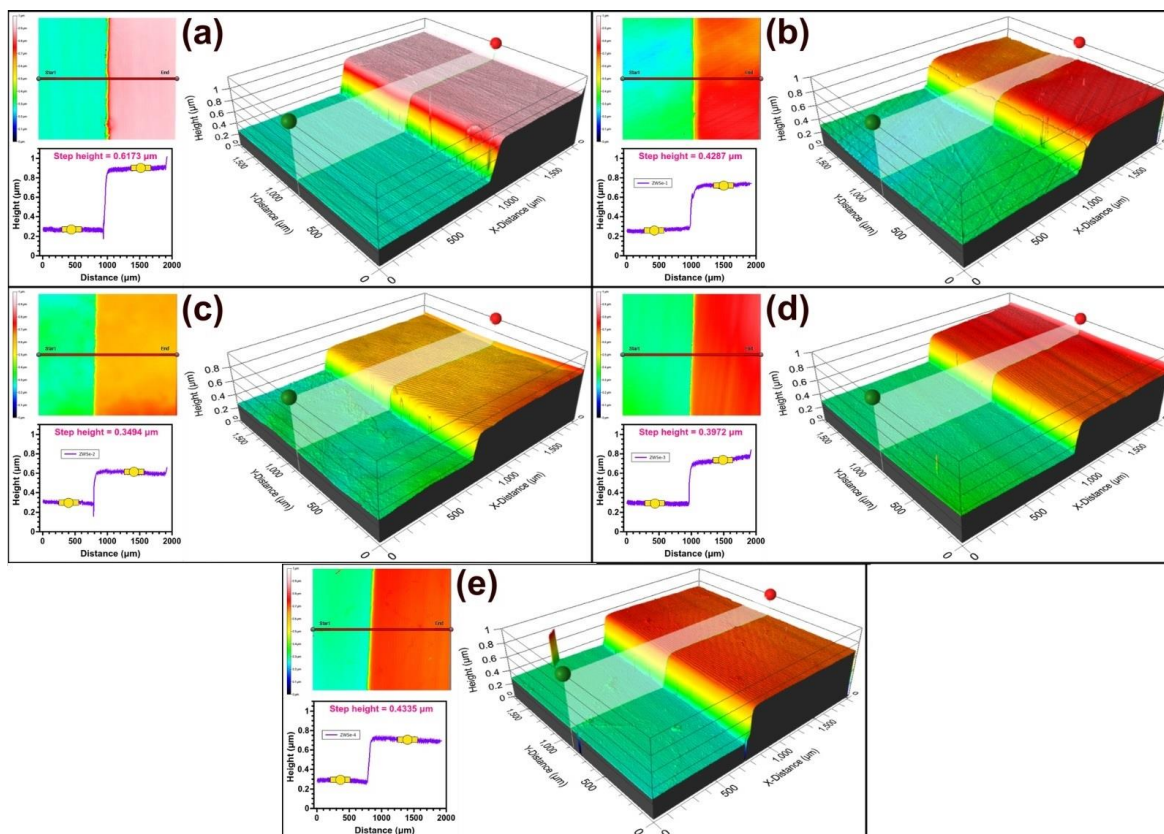


**Fig. S1.** Optical profilometer images of pristine WSe<sub>2</sub> CE and ZnWSe<sub>2</sub> alloy CEs. (a) WSe<sub>2</sub>, (b) ZnWSe<sub>2</sub>-1, (c) ZnWSe<sub>2</sub>-2, (d) ZnWSe<sub>2</sub>-3 and (e) ZnWSe<sub>2</sub>-4 alloys.

### Supplementary Note-1:

Figure S1 shows the 2-dimensional (2D) and 3-dimensional (3D) surface images and film thickness graphs of pristine WSe<sub>2</sub> CE and ZnWSe<sub>2</sub> alloy-based CEs obtained by the optical interference method. In the graphs obtained from the 3-dimensional image, the average difference between the two levels gives information about the thickness of the thin film. As shown in Fig. S1(a), the thickness of pure WSe<sub>2</sub> thin film was determined as 0.62 μm. Such thickness can be ascribed to the presence of vertically grown nanosheet structures on the substrate as illustrated in FESEM images. As displayed in Fig. S1(b), the formation of WSe<sub>2</sub> nanosheets was disrupted and collapsed substantially with the incorporation of Zn atoms into the WSe<sub>2</sub> structure. The measured thickness was determined as 0.43 μm, revealing a rapid decrease in the thickness of ZnWSe<sub>2</sub>-1 CE. The ZnWSe<sub>2</sub>-2 sample shown in Fig. S1(c) had the least thickness among the grown thin films. As can be seen from the FESEM images, the nanosheet is no longer on the surface and the film has turned into a completely different form. Therefore, the film thickness was determined as 0.35 μm. The thickness of the ZnWSe<sub>2</sub>-3 thin film shown in Fig. S1(d) was measured as 0.40 μm. The thickness of the ZnWSe<sub>2</sub>-4 thin film shown in Fig. S1(e) was also measured as 0.43 μm. The reason for the increase in thickness is to increase the power of the Zn metal target material while keeping the sputtering power of the WSe<sub>2</sub> target material constant. Because the amount of atoms coming on the substrate in unit time is increasing gradually and these atoms are deposited on the substrate in amorphous form.

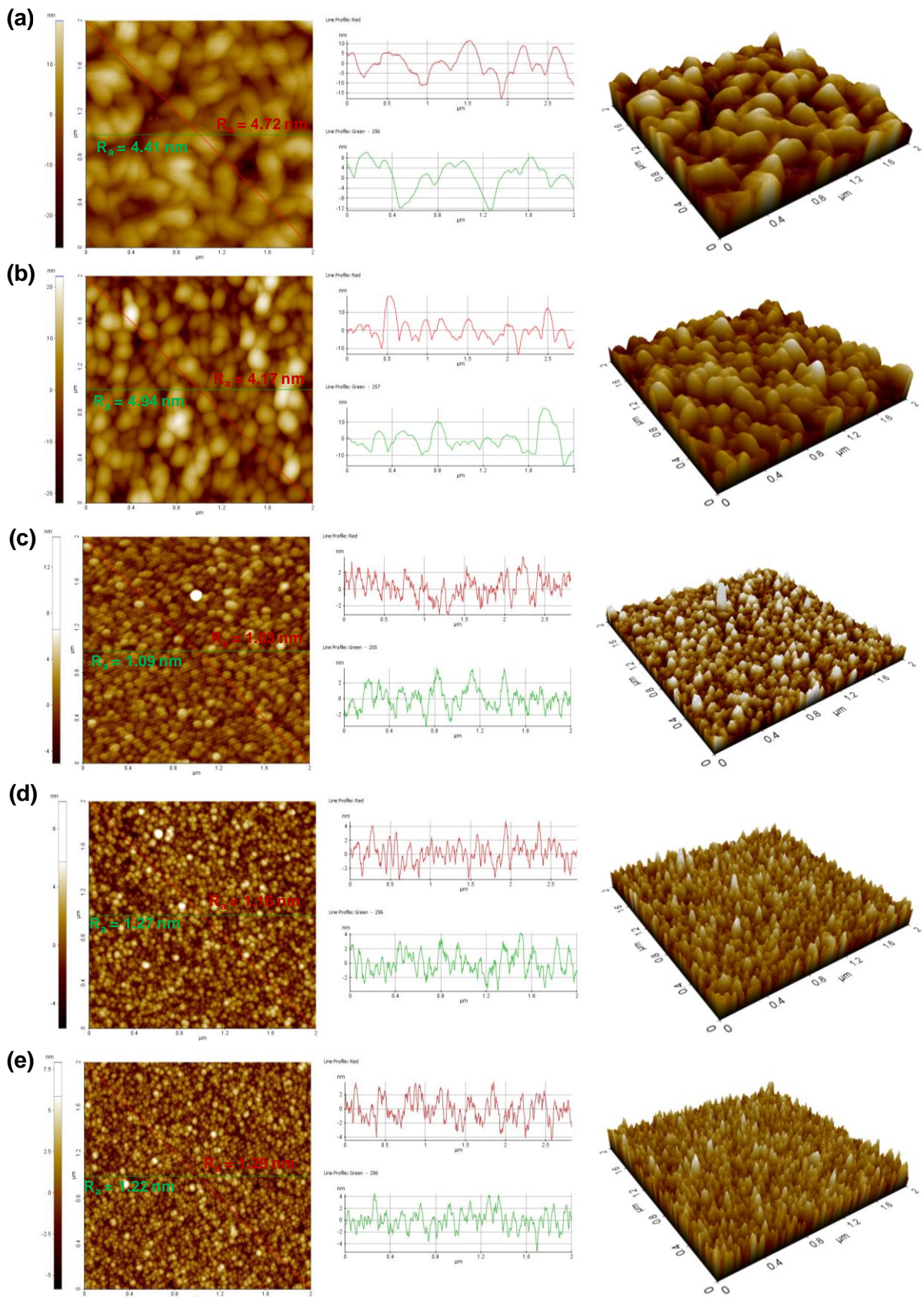


**Fig. S2.** 2D/3D AFM images and line roughness profiles of (a) WSe<sub>2</sub>, (b) ZnWSe<sub>2</sub>-1, (c) ZnWSe<sub>2</sub>-2, (d) ZnWSe<sub>2</sub>-3 and (e) ZnWSe<sub>2</sub>-4 alloys.

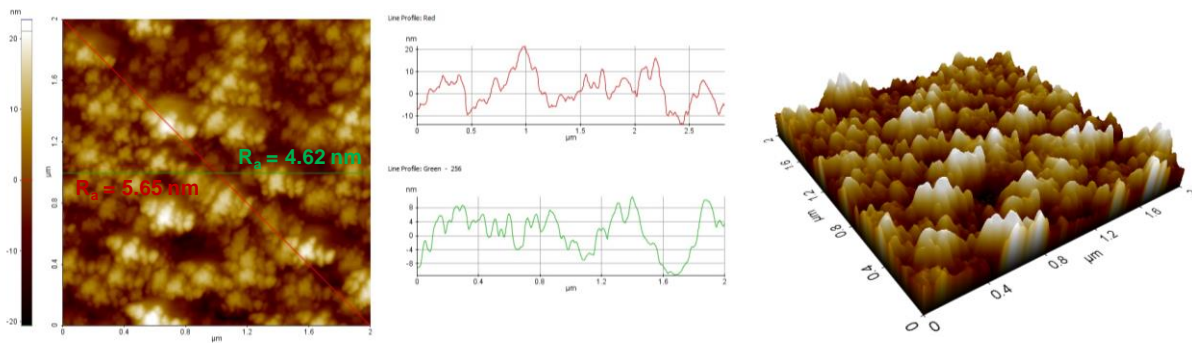


**Fig. S3.** 2D/3D AFM images and line roughness profiles of Pt CE.



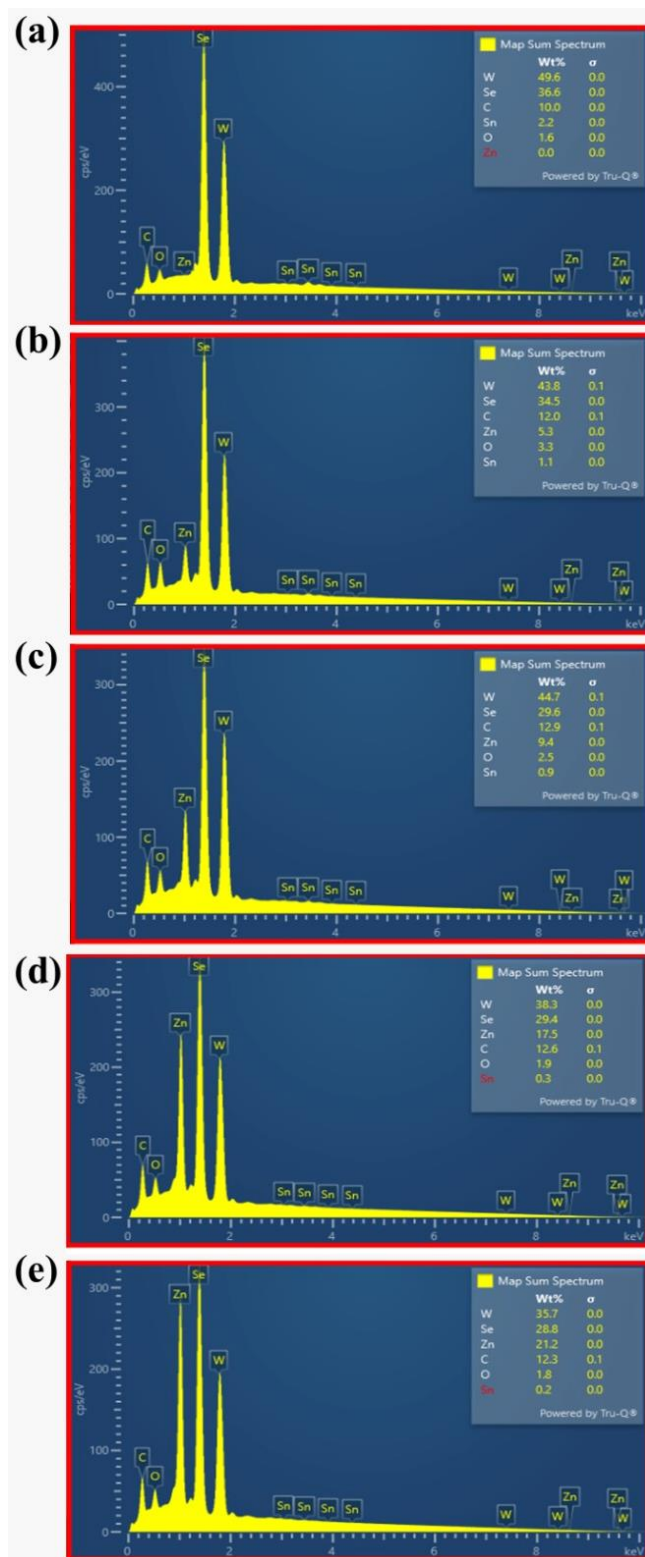


**Fig. S4.** EDX spectrum and weight composition ratios of pristine WSe<sub>2</sub> CE and ZnWSe<sub>2</sub> alloy CEs. (a) WSe<sub>2</sub>, (b) ZnWSe<sub>2</sub>-1, (c) ZnWSe<sub>2</sub>-2, (d) ZnWSe<sub>2</sub>-3, and (e) ZnWSe<sub>2</sub>-4 alloys.

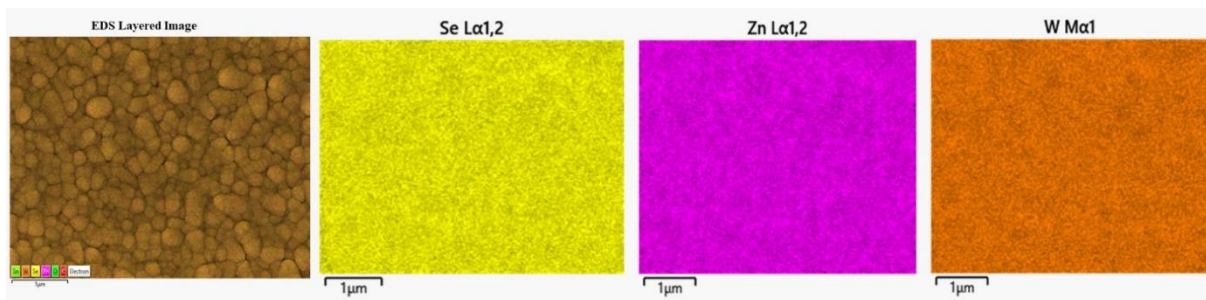


**Fig. S5.** Elemental mapping for Se, Zn and W of ZnWSe<sub>2-3</sub> sample.

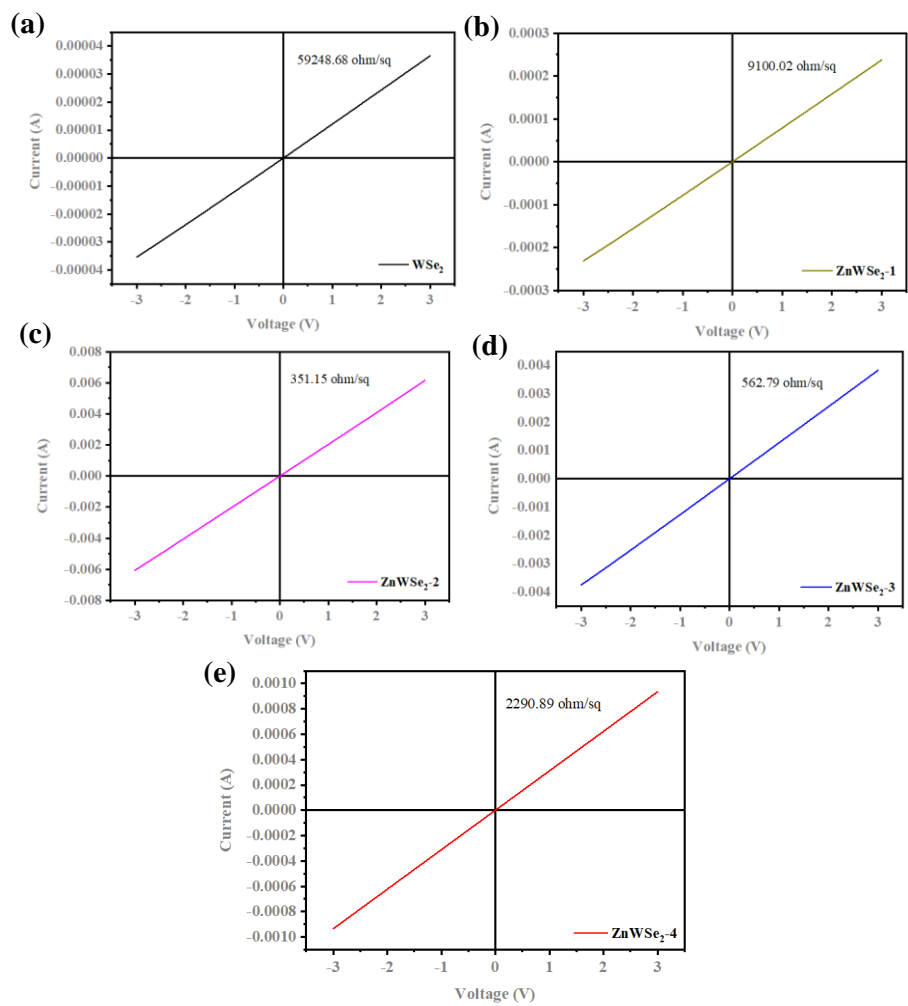


**Fig. S6.** I-V curves of all WSe<sub>2</sub> and ZnWSe<sub>2</sub>-based samples collected in ambient conditions.



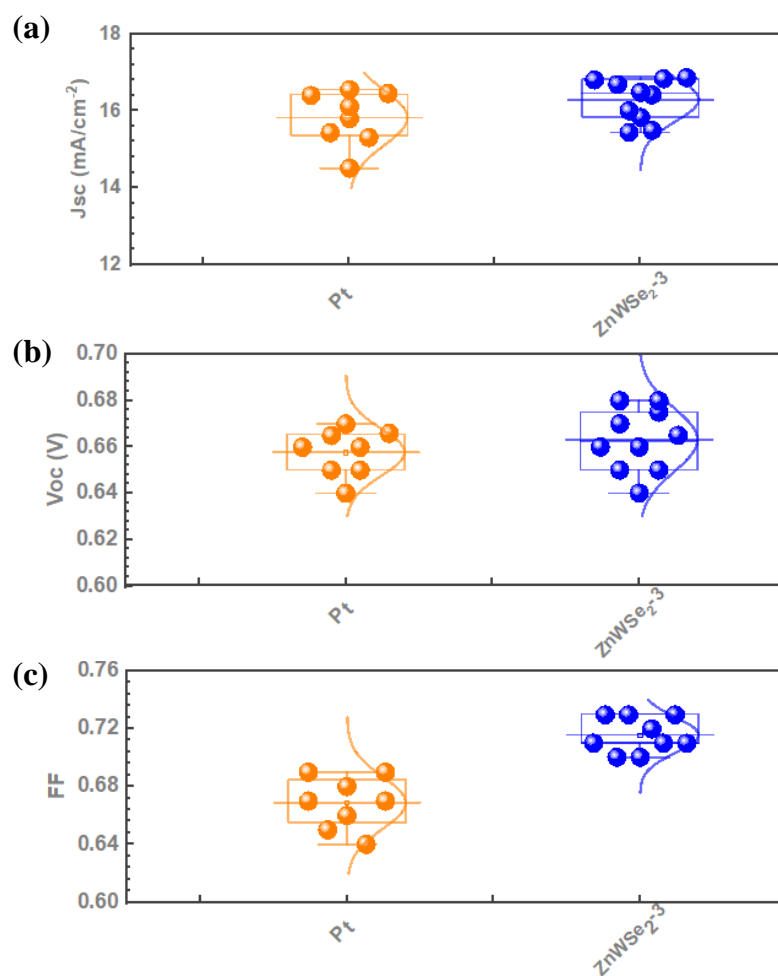


**Fig. S7.** The histograms of individual devices of (a)  $J_{sc}$ , (b)  $V_{oc}$  and (c) FF of DSSCs employing Pt and ZnWSe<sub>2-3</sub> CEs.

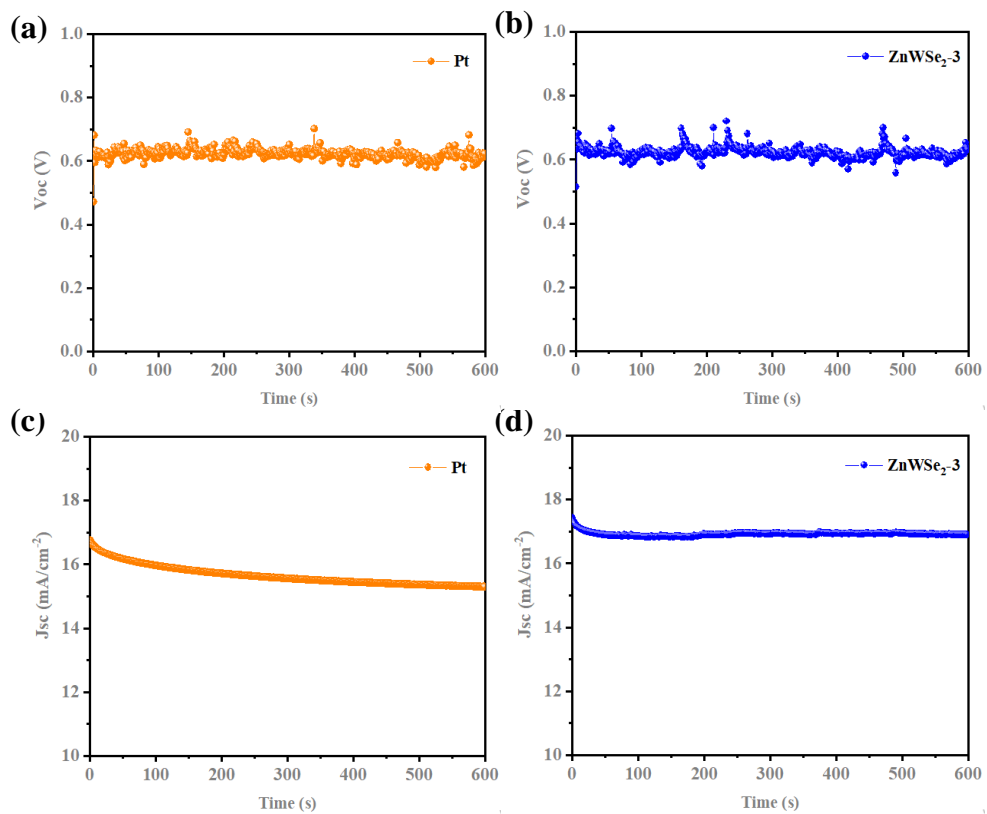


**Fig. S8.** The  $V_{oc}$  (a,b) and  $J_{sc}$  (c,d) curves of the cells as a function of time. (a,c) Pt and (b,d) ZnWSe<sub>2</sub>-3 CE-based cells.

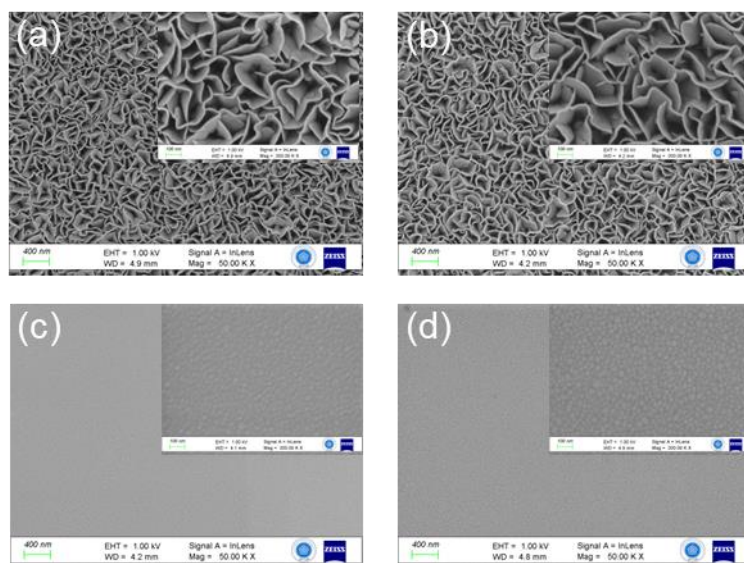


**Fig. S9.** The FESEM images of the (a, b) pristine WSe<sub>2</sub> and (c, d) ZnWSe<sub>2</sub>-3-based CE films before (a, c) and after (b, d) electrolyte immersion during 120 h.